Biomedical Engineering Advances 7 (2024) 100119

Contents lists available at ScienceDirect

Biomedical Engineering Advances

journal homepage: www.journals.elsevier.com/biomedical-engineering-advances

A new height contouring method for severity prediction in cam-type hip joints: 20 subject-specific cases

Trent Edward Rayment *, Sophie Williams, Alison Claire Jones

Institute of Medical and Biological Engineering, School of Mechanical Engineering, University of Leeds, Woodhouse Lane, Leeds LS2 9JT, United Kingdom

ARTICLE INFO

Keywords:
Femoroacetabular impingement
Cam lesion
Shape model
Severity prediction
Contour

ABSTRACT

Cam-type femoroacetabular impingement syndrome (FAIS) is characterised by a non-spherical continuation of the femoral head into the femoral head-neck junction and is associated with damage to the acetabular cartilage. Diagnostic methods based on cam shape are progressing from 2D radiographic measurements to 3D CT measures, providing greater insight. There is currently no consensus on how to describe the 3D cam lesion shape and subject-specific impingement mechanisms are difficult to determine.

A novel 3D 'contour' method was used to describe the proximal femur of 20 cam-type hips. Five contours, analogous to height contours on a terrain map, were used to describe the femoral head-neck junction, capturing the progressive height of the cam lesion. From that description, the *cam apex* (a subject's largest alpha angle), *cam extent* (spread around the femoral head), *cam location* (position around the femoral head) and *average acetabular coverage*, were recorded. A previously developed hip impingement model was used to apply 126 activity-based motions to each subject-specific hip shape and predict impingement occurrence and depth of incursion past the acetabular rim. Correlations between shape measures and impingement occurrence were investigated.

The two contours representing the lowest heights (close to the head best fit sphere and 1 mm greater than that) generated cam alpha angle and cam extent measurements which contained the typical clinical measures (Alpha: close to best fit 47°-98°, at 1 mm 45°–77°; Extent: close to best fit 0°–129°, at 1 mm 0°–100°). The remaining contours described the progressive height of the cam lesion up to 4 mm greater than the head radius. Impingement was predicted predominantly from the first 1 mm height of the cam, with only two subjects impinging at a cam height greater than 2 mm. Therefore, it is possible that adequate resection of the first 1 mm of cam height is the most critical in reducing a subject's impingement severity.

Impingement occurrence was positively correlated with the cam apex ($\rho = 0.84$ close to best fit, $\rho = 0.70$ at 1 mm height), the cam extent ($\rho = 0.68$ close to best fit, $\rho = 0.80$ at 1 mm height) and the acetabular coverage ($\rho = 0.50$, at 1 mm height). However, in line with other work on cam impingement, correlations between any single shape measure and the risk of impingement were not strong enough to be used with confidence as predictive tools. This supports the further development of modelling tools which sufficiently capture the complex shape and can generate an impingement risk metric which accounts for joint motion.

Introduction

Femoroacetabular impingement syndrome (FAIS) is associated with abnormal geometry of the hip joint, leading to pain and reduced mobility, and has been shown to increase the chances of developing osteoarthritis in later life [1]. Cam-type FAIS is characterised by a nonspherical continuation of the femoral head into the head-neck junction of the femur. Surgical intervention for cam-type impingement has increased over recent years, with over 7000 cam removal surgeries reported by the non-arthroplasty hip registry in the UK in 2022, more than twice as many completed in 2018 [2]. It is thought that repeated high-pressure contact between the femoral bone and the acetabular rim leads to damage of the soft tissues in the acetabulum. Typically, cartilage damage occurs in the superolateral and anterior peripheral areas of the

Abbreviations: 2D, Two-dimensional; 3D, Three-dimensional; CAD, Computer Aided Design; CT, Computed Tomography; FAIS, Femoroacetabular Impingement Syndrome.

* Corresponding author.
E-mail address: mntr@leeds.ac.uk (T.E. Rayment).

https://doi.org/10.1016/j.bea.2024.100119
Received 21 December 2023; Received in revised form 6 March 2024; Accepted 18 March 2024
Available online 19 March 2024
2667-0992/

acetabular and often includes delamination of the cartilage from the subchondral bone [3].

Definition of cam lesion shape varies between studies, with most reporting in terms of the largest *alpha angle*, a two-dimensional (2D) measure that quantifies the sphericity of the femoral head-neck junction, at a location dependent on the radiographic view [4]. More comprehensive three-dimensional (3D) measures of cam lesion shape have been shown to impact impingement severity, for example there is a link between a larger spread of the cam lesion around the femoral neck (*extent*) and larger areas of acetabular cartilage damage [5]. Additionally, cam volumes have been shown to predict the extent of soft tissue damage more reliably than two-dimensional (2D) measures such as alpha angles [6]. Current 3D methods that capture cam shape describe variations in cam height [7,8], but do not capture a full shape description of the femoral head-neck junction and are hard to compare to the current clinical 2D indicators used for assessing impingement severity (namely maximum alpha angles). There is currently no consensus on which 3D measures are most useful and none of those tested to date encompass the increase in femoral head radius in the cam region.

Diagnosis of FAIS is challenging as cam features visible on radiographs are common in asymptomatic subjects, and evidence can be subtle, requiring further physical assessment to confirm a diagnosis [9]. While particular movements are associated with cam-type impingement, subject-specific impingement mechanisms are difficult to determine.

A computationally low-cost shape-motion model, capable of generating impingement severity measures for hip shapes over a range of different activities, has previously been demonstrated on idealised cam-type hips based on published cam shape data [10]. However, this model has not been assessed in terms of its ability to differentiate predicted impingement in a set of real cam-type FAIS subjects and its current functionality is limited to only tracking the impingement of the leading edge of the cam lesion.

The overall aim of this work was to use a 'contour' description of the progressive height of the cam lesion of 20 cam-type hip joints and modify an existing shape-motion model to assess the occurrence of impingement for multiple cam lesion height contours. The specific objectives were: 1) to describe the shapes of 20 cam hips using the contour method and extract shape measurements aligned with previous work; 2) to determine the spread of impingement severity measures across the 20 hips, using the modified shape-motion model; 3) to test the hypothesis that a common cam shape metric can be used in isolation to anticipate predicted impingement occurrence.

Materials and methods

Overview of study design

Subject-specific 3D shape models were generated from CT scans for 20 patients with clinically diagnosed cam-type hips (10 of male sex and 10 of female sex, age range 22–49 years). The CT data was collected and available for reuse from a previous study (ethical approval: MEEC 11–044, Faculty of Engineering Research Ethics Committee, University of Leeds, UK).

A new 3D shape capture method was developed and used to describe the height profile of the femoral head-neck junction, including the cam lesion (Fig. 1, orange boxes). The method used five contours, analogous to height contours on a terrain map, each defined as a set of points around the femoral head-neck junction. The acetabular rim shape was defined by a single set of points describing the coverage of the bony rim. Derivative measures of cam extent, cam location, cam apex size, and mean acetabular coverage angle were taken for quantification.

For each subject-specific hip shape, the shape-motion modelling process from a previous study was followed [10] (Fig. 1, blue boxes). In brief, the femoral and acetabular shape descriptions were aligned in 3D space and 126 motions cases were simulated, generating various measures of impingement severity. Unique to this work, the process was repeated for each of the five contours of the femoral head-neck junction, representing different heights of the cam lesion.

Finally, correlation analysis was performed to assess any relationships between hip shape measures and the predicted occurrence of impingement.

Subject-specific source data

Data collection was completed from 3D models of the proximal femur and acetabular socket of 20 cam-type hips using CAD software (SolidWorks, Dassault Systems, San Diego). The geometry had been previously segmented in 3D image processing software (ScanIP, Synopsys, Sunnyvale CA) from CT images (voxel size 0.7422 × 0.7422 × 1 mm) [11].

Femoral head-neck junction data collection

The 3D shape of the femoral head-neck junction was described, by five sets of points, each set representing a 'contour'. Each contour was established using spheres centred at the femoral head centre and by finding locations where the femoral head-neck junction protruded from

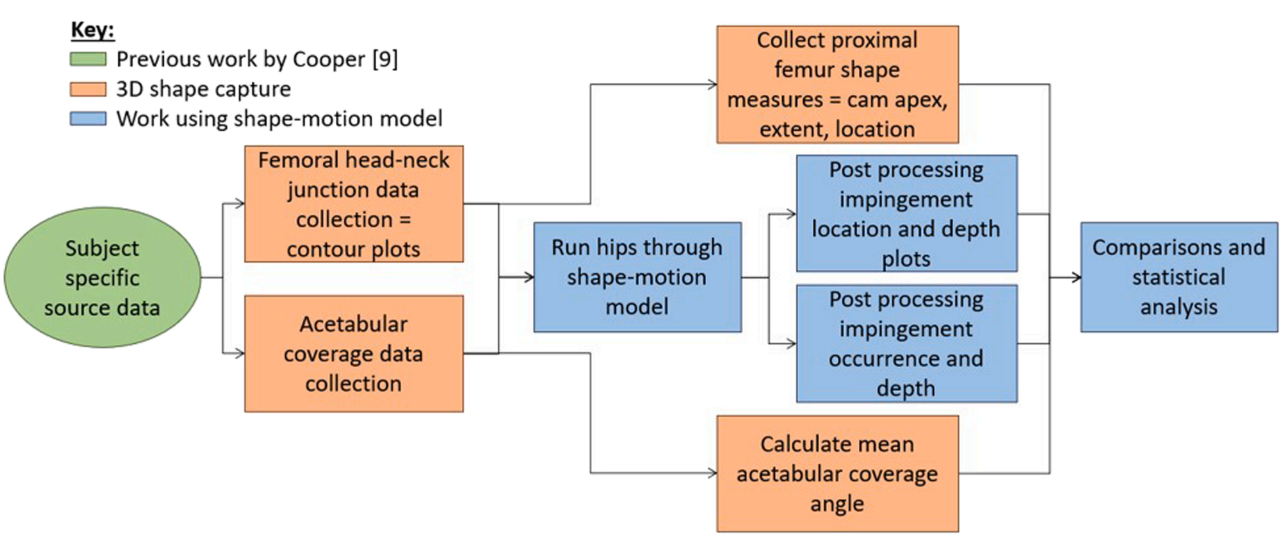

Fig. 1. Workflow of the methods used in this study. Previous work completed by Cooper [9] segmenting 3D hip models from CT scans. **Colour to be used in print.**

that sphere. The first 'contour sphere' was determined by generating a sphere of best fit for the 3D segmented model of the femoral head and then expanding the radius by 0.35 mm to encompass the natural non-uniform surface of the femoral head. The further four spheres were generated by expanding the radius in intervals of 1 mm from the original best fit sphere (i.e., +1 mm, +2 mm, +3 mm, +4 mm) (Fig. 2A). Including a sphere of +4 mm ensured that areas of the cam with a height equivalent to an average joint space were captured [12]. The femoral neck axis was found by determining the centre of the thinnest point of the femoral neck and projecting it through the femoral head centre. Along the line where each sphere intersected the neck-head junction, 24 points were recorded equidistant around the femoral neck axis (Fig. 2B). For each point on a contour an angle was recorded (e.g. angles α_{00} and α_{06} in Fig. 2A), defined as the angle between the femoral neck axis and a line from the femoral head centre to the point at which the relevant contouring sphere intersected the segmented femoral surface (Fig. 2C). Like elevation contours on a terrain map, each of these represented the boundary where the femoral head-neck junction protrudes out of a particular sized sphere (Fig. 2C). These angles are similar in nature to clinically measured alpha angles [4].

Acetabular coverage data collection

The acetabular coverage was described by angles taken from 21 equidistant points around acetabular rim, excluding the acetabular notch area (Fig. 3A). The outward facing axis (Fig. 3B) was computed from a plane determined by the two points either side of the acetabular notch, and the most superior point of the acetabular rim, projecting from this plane through the joint centre. Angles were measured between a line connecting the 21 points on the acetabular rim with the joint centre, and the outward facing axis (angles α_{03} and α_{09} in Fig. 3B) to produce the acetabular coverage plot (Fig. 3C).

Computational shape-motion model output measures

The computational model, combining hip joint shape and motion, was implemented in Matlab (R2023a The Mathworks Inc) [10]. To establish the joint orientation, the femoral contour points and

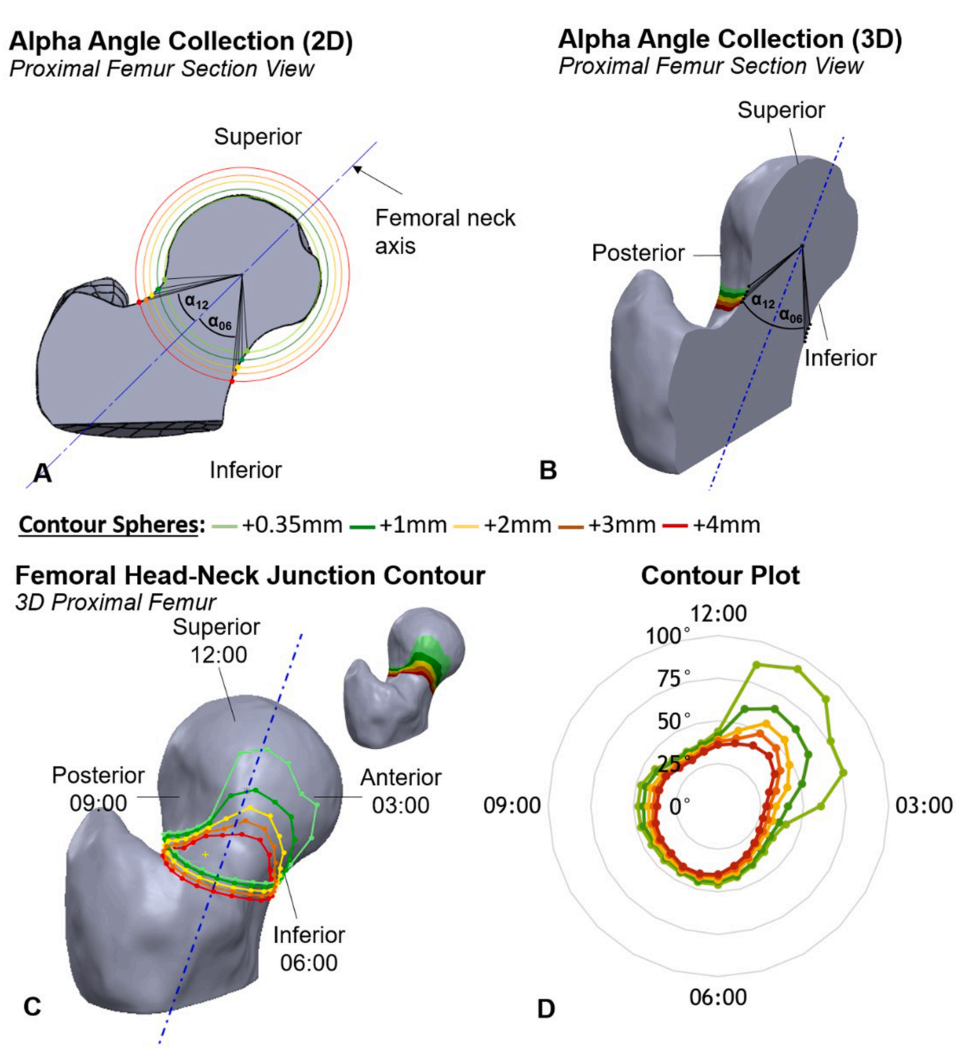

Fig. 2. Visualisation of the femoral head-neck junction data collection. A) All five contouring spheres on a 2D slice of the proximal femur, showing example alpha angle measurements collected at the superior (12:00) and inferior (06:00) clock face positions. B) All five contouring spheres on a 3D view of the proximal femur, showing example alpha angle measurements collected at the superior (12:00) and inferior (06:00). The colour bands in the posterior locations of the femoral head-neck junction illustrate the areas between the contour boundaries. C) Projection of the points at which the angles are measured around the femoral neck onto the 3D model and visualisation of the different contour boundaries on a 3D model. D) A contour plot of the measured angles at each of the 24 locations about the femoral neck. The clock plot is from a view looking directly up the femoral neck in a medial direction, with the centre point aligning with the femoral neck axis.

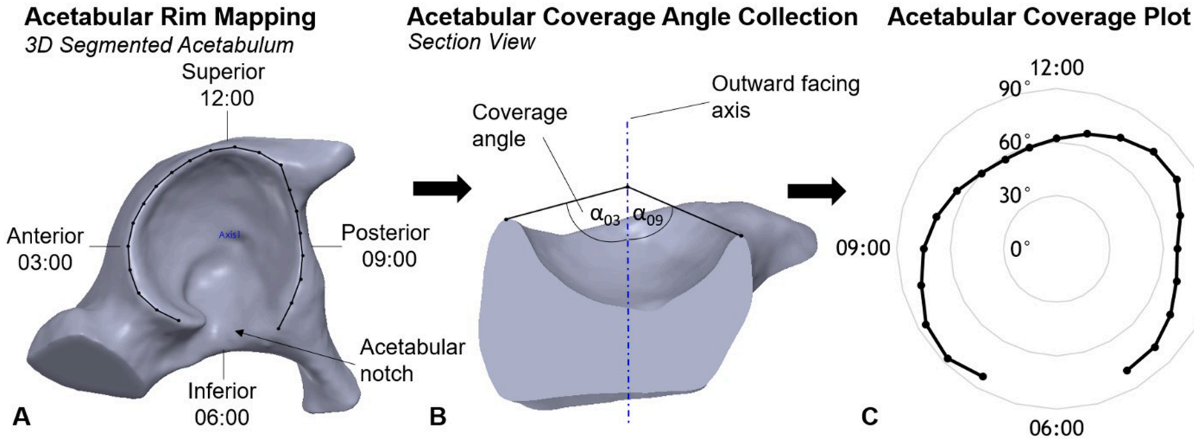

Fig. 3. Visualisation of acetabular coverage angle collection method; A) Example of two coverage angles at 03:00 and 09:00; B) projection of the points at which the angles are measured around the acetabular rim; C) a plot of the coverage angles at each of the 21 locations about the femoral neck.

acetabular rim points were aligned in the same 3D coordinate system (an example of a singular set of contour points and the acetabular rim is shown in Fig. 4A). As subject-specific hip alignment was uncertain, the same typical neutral alignment was used for all subjects, which was established in previous work from FAIS and control populations [10].

The shape-motion model was used to simulate each joint through a total of 126 motion cases. Any interference of the femoral contour points with the acetabular rim points during simulation indicated impingement had occurred (Fig. 4B). In order to make a comparison of impingement risk across the different hip shapes, the same set of motions were applied to all hips. This approach meant that impingement measurements could be directly compared between hip shapes. (This is in contrast to the application of subject-specific motions, which would introduce an additional confounding factor.) The hip motion data set was comprised of 14 different activity motions, performed by nine individuals, representing an envelope of possible pain-free motion of the human hip. Briefly, the motions included six daily activities (e.g. walking and sit to stand), five higher flexion activities (e.g. squat and cycling) and three activities with higher internal/external rotation (e.g. a leg cross and golf swing). The volunteers were from the general population (age range 20–70 years, mean age 44 years) and were free of mobility impairing conditions [13]. Of the 126 motion cases, 61 were from males and 65 were from females. Details of the selection of those motions are available in an open data set [14].

For each combination of hip shape subject, the measures derived from the model were impingement occurrence, impingement depth, and location of impingement. Impingement occurrence was defined as the total number of motion cases in which impingement was predicted, out of a possible 126 for each contour. When incidences of impingement occurred, the depth of the impingement was tracked (Fig. 4B). This was

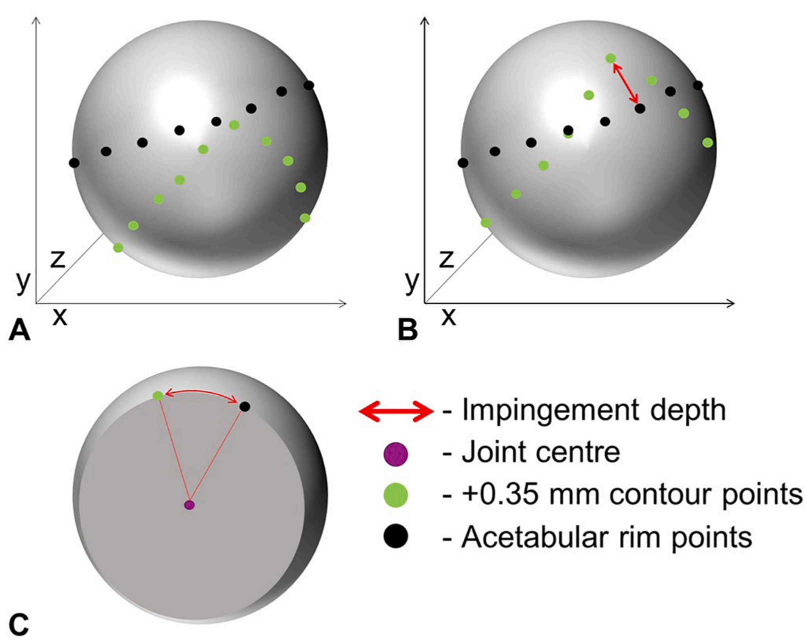

Fig. 4. An example of the acetabular rim points and a single set of femoral contour points in the same 3D coordinate system for one subject, shown on a 3D unit sphere. A) Shows the hip before applying a motion case, in the neutral hip alignment position. B) Example of a motion case, applied to the same hip in A, whereby impingement has occurred, indicated by the green points of the +0.35 mm contour passing through the black points of the acetabular rim. The red arrow between the contour point and acetabular point represents the impingement depth measure. C) A 2D representation of the measurement of the deepest impinging point of the +0.35 mm contour, from the motion case applied in B, whereby the impingement depth is measured as the angle between the deepest impinging point of the +0.35 mm contour sphere and nearest point of the acetabular rim, from the joint centre.

defined as the angle between each of the impinging femoral contour points and the points defining the acetabular rim (Fig. 4C). The maximum angular depth was recorded for each impinging motion case. The occurrence and depth measures were recorded separately for each of the five sets of contour points.

To show the location of impingement on the acetabular, the impingement depth information was mapped into an idealised clock plot representing the acetabular socket. By overlaying each impinging motion case for each femoral head-neck junction contour onto a singular plot, a subject could be qualitatively assessed for the focal point of impingement.

Cam lesion shape features

Three shape measures were taken from the cam contour description: cam extent, cam location and cam apex. Cam extent was calculated as the angular spread of the cam around the femoral neck axis, at an alpha angle threshold value of 50°, for the +0.35 mm and the +1 mm contours (Fig. 5A) (adapting the method described in work by Mascarenhas, et al. [5]). Cam location was defined by measuring the position of the centre point of the cam extent, taken as an angle anticlockwise from the anterior (Fig. 5B). Cam apex was determined by a subject's largest measured alpha angle, which by definition falls on the +0.35 mm contour (Fig. 5C).

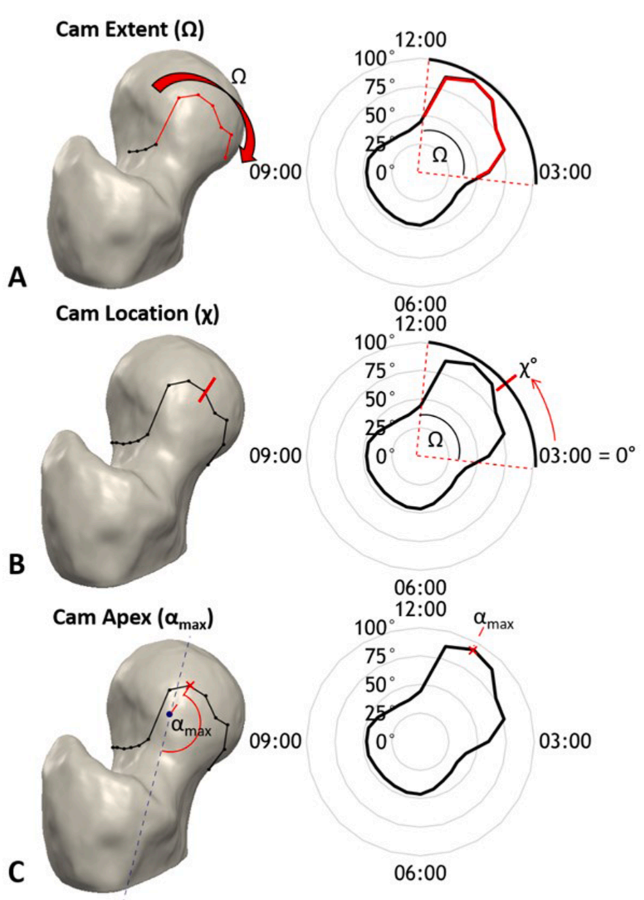

Fig. 5. A) Measurement of cam extent, where measured angles (highlighted in red) are above the threshold angle indicative of cam-type features. B) Measurement of cam location, taken from the centre point of the cam anticlockwise from the anterior of the model to the centre of the cam extent. C) Measurement of cam apex, the maximum measured femoral head-neck junction angle of a subject.

Comparisons and statistical analyses

Contour plots describing the femoral head-neck junction for all 20 subject specific hips were produced, allowing for qualitative assessment of the range of cam shapes. The shape was quantitatively assessed through the range and distribution of the cam apex, cam location, and cam extent.

The impingement results from the shape-motion model for all five contours, were overlaid on plots illustrating impingement location around the acetabulum. The severity of predicted impingement was described by the occurrence and depth measures. Impingement occurrence measures were recorded out of a possible 126 occurrences of impingement [10] for each of the five contours, totalling a possible 630 occurrences of impingement for each subject. To avoid over interpretation of individual combinations of joint shape and motion, results with less than three occurrences of impingement were not used for further analysis.

The maximum impingement depth for each motion case was recorded for the +0.35 mm contour. The average and standard deviation of the maximum impingement depths were then calculated for each activity. The depth data for a particular activity was excluded from further analysis where less than three motion cases were predicted to impinge for a single activity. The average impingement depth for each subject was computed from the activity level data. For ease of data interpretation, the depth measurements (in degrees) were converted to millimetres by assuming a femoral head radius of 25 mm.

To assess the effects of an individual's cam shape on predicted impingement, relationships between the shape features and impingement occurrence were investigated. The cam apex, cam extent and cam location measurements were compared with the impingement occurrence from the +0.35 mm contour and from the +1 mm contour, using a Spearman's rank coefficient (ρ) (Contours with insufficient levels of impingement occurrence were not included in the correlation analysis).

To investigate the relationship between acetabular coverage and impingement occurrence, the mean acetabular coverage angle was calculated for each subject. Mean coverage angle was compared to impingement occurrence from the +0.35 mm contour and the +1 mm contour, using a Spearman's rank coefficient.

Results

The data associated with this paper is openly available from the University of Leeds Data Repository [15].

Contour description of 20 subject specific hips with cam lesions

The contour description of the cam lesions illustrates the variation cam 'height' profile, expressed through the distance between the contour lines (Fig. 6). For example, Subject 10 had small differences in angles between contour lines, depicting a cam with a steep height gradient. This is in contrast with Subject 05, with larger differences in angles between the contour lines, depicting a cam with a lower height gradient across the head neck junction. A very large cam would be indicated by a large apex angle (pale green, near the edge of the plot) and with the contours close together, indicating a steep change in height near the articular surface.

The cam shape measures, taken using the +0.35 mm contour, were as follows. All subjects recorded at least one angle value greater than 50°, indicative of cam morphology, except for Subject 20 (Fig. 6). The cam apex ranged from 47°–98°, with a mean maximum angle of 75° The average cam location was 34.4° (anticlockwise from the anterior, Fig. 5B) with a range of 7.5°–52.5° The cam extent (using an alpha angle threshold value of 50°) ranged from 0° (Subject 20) to 129° (Subject 14), with an average of 80°

In the subsequent contours representing greater heights of cam lesion, (1 mm, 2 mm, 3 mm and 4 mm), there were fewer points for

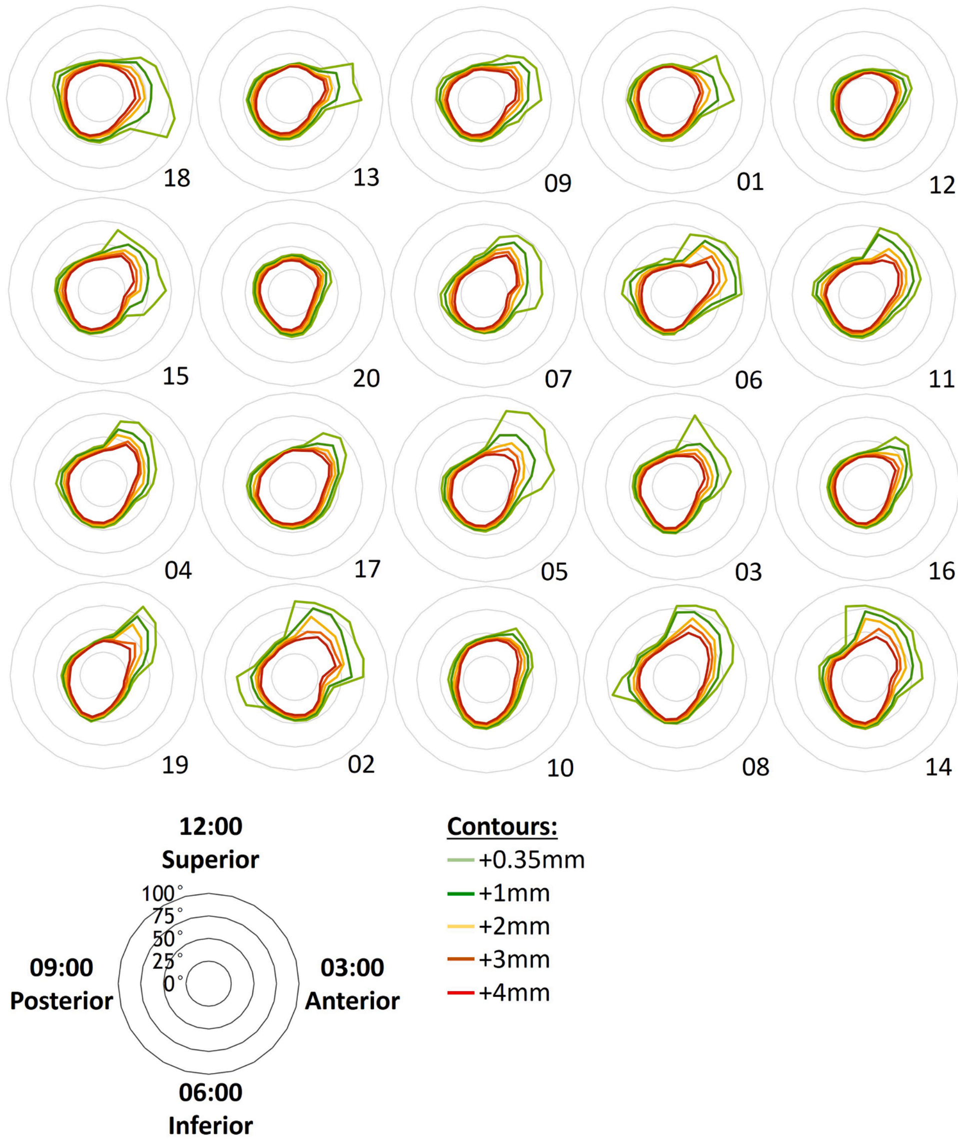

Fig. 6. Contour plots of subject-specific femoral head-neck junctions. The numbers against each plot are the subject codes. The plots are given in order of cam location from the most anterior at the top left, moving along each row in turn to the most superior at the bottom right.

which the alpha angle exceeded 50° The cam shape measures taken at the +1 mm contour were as follows. The range of the cam apexes was 45° – 77°, with an average of 61, and 19 subjects had a cam apex exceeding 50° The cam extent ranged from 0° (Subjects 01, 12 & 20) to 100° (Subject 02), with an average of 53° Shape measures for the contours of increasing height displayed further decreases in cam apex, and cam extent, with each subsequent contour sphere. The maximum alpha angle recorded in the +4 mm contour for any subject was 49°, as shown by the red contours in Fig. 6.

Two subjects (08 and 02) displayed angles exceeding the 50° threshold in the posterior area, indicating larger heights of the femoral head-neck junction were present.

Assessing the range and distribution of impingement occurrence, depth, and location across 20 cam-type hips

Impingement was predicted predominantly from the +0.35 mm contour in the superior edges of the acetabular, with some subjects, such as 18, predicting more anterior impingement (Fig. 7, pale green lines). In all hips, impingement was predicted posteriorly due to a single motion case from a single activity. This has been left in the plots of completeness but as this is a single motion case, it is not considered a significant result and is removed from the quantitative analysis of the impingement depth.

Total impingement occurrence for a subject's hip, ranged from a low of 5/630 to a high of 94/630 (Fig. 8). The 20 subjects produced a mean impingement occurrence of 24/630 for all contours combined. As expected, higher impingement rates were predicted for the +0.35 mm contour than any other, ranging from 2/126 to 86/126.

The contour specific impingement occurrence data provide an indication of severity (Fig. 8). Subject 18 impinged in many motion cases with the shallowest part of the cam lesion (86/126 with +0.35 mm contour), but impingement with the higher parts of the cam happened in only a small number of motion cases (3/126 with +1 mm contour) and has no significant impingement where the cam height exceeded the head radius by 2 mm or more. Two subjects (08 and 19) have cases of impingement which reach parts of the cam 2–3 mm greater in height than the head radius and no subjects impinged in areas with heights greater than 3 mm.

Six subjects did not meet the impingement occurrence criteria to allow an average maximum depth to be computed; subjects 01, 09, 10, 12, 16 and 20. Subject 17 had three occurrences of impingement for a single activity and therefore sufficient data for depth approximation.

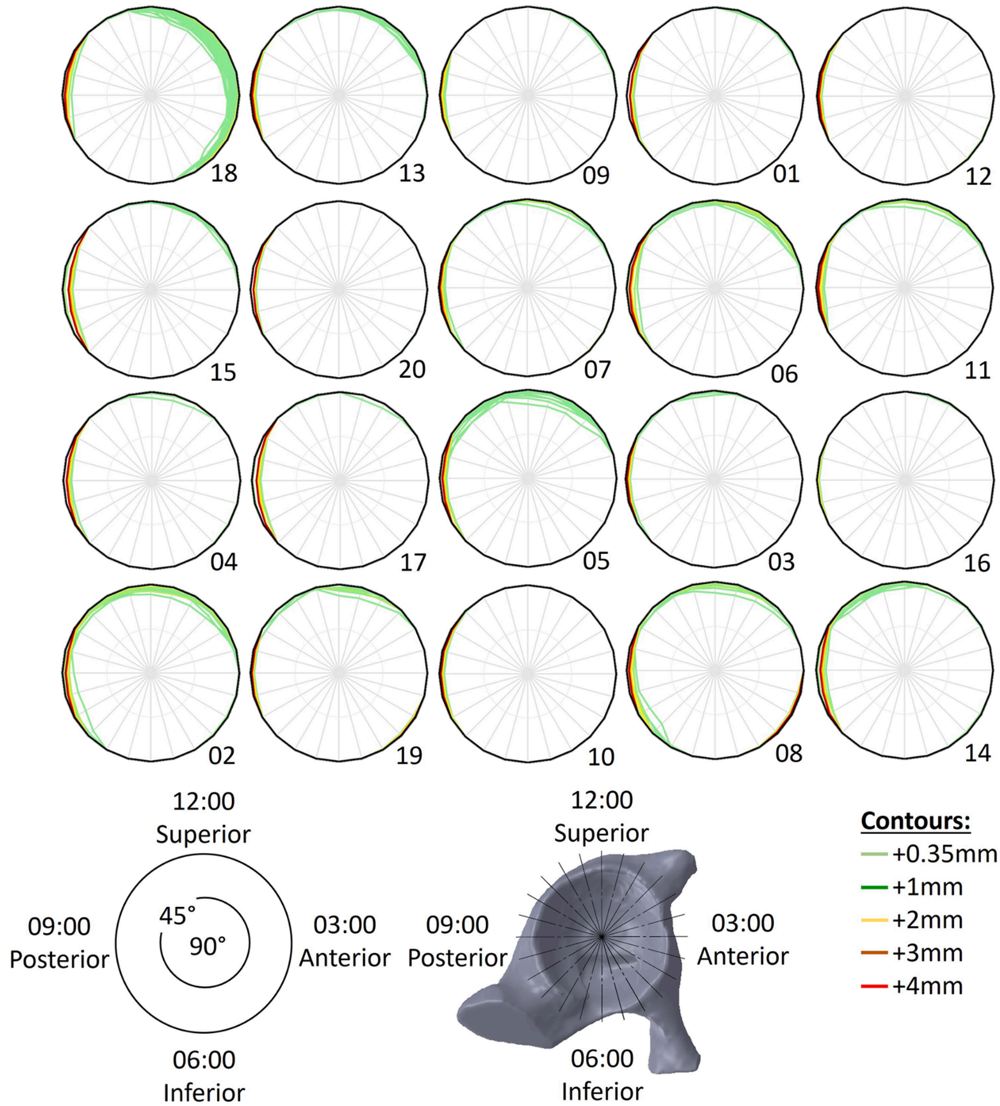

Fig. 7. Predicted acetabular impingement plots for all 20 subjects. For each impinging motion case, the plot displays the largest angle that any cam point reached into the acetabular, at each point around its rim. The plots are given in order of cam location from the most anterior at the top left, moving along each row in turn to the most superior at the bottom right.

	Subject Code:	18	02	06	08	05	13	15	14	19	11	03	07	04	09	01	17	10	12	20	16
Contour	+0.35	86	46	31	28	26	24	18	16	14	11	8	8	6	6	5	5	2	2	2	2
	+1	3	11	8	6	2	1	4	5	3	3	2	3	3	1	1	1	2	2	1	1
	+2	2	2	2	3	1	1	1	1	3	2	1	1	1	1	1	1	1	1	1	1
	+3	2	1	1	2	1	1	1	1	2	1	1	1	1	1	1	1	1	1	1	1
	+4	1	1	1	2	1	1	1	1	2	1	1	1	1	1	1	1	1	1	1	0
	SUM	94	61	43	41	31	28	25	24	24	18	13	14	12	10	9	9	7	7	6	5

Fig. 8. Impingement occurrence out of a possible 126 for each of the femoral head-neck contours for each of the 20 subject-specific hips. Impingement occurrence is coloured on a scale whereby red indicates high occurrences of impingement, reducing to lower occurrences of impingement from orange through to light yellow. Areas in grey indicated an occurrence of less than 3.

Average maximum impingement depths for each of the remaining 14 subjects, using the +0.35 mm contour, ranged from 2 mm ± 1 mm to 5 mm ± 3 mm (with an overall average of 3 mm ± 2 mm).

Distinguishing patterns of predicted impingement occurrence with cam apex, location, and extent

There was a strong correlation between cam apex size and impingement occurrence for the +0.35 mm contour (ρ = 0.84). The correlation between cam apex size and impingement occurrence for the +1 mm contour was naturally lower (ρ = 0.70), as the maximum cam apex will always lie on the +0.35 mm contour (Fig. 9A).

Impingement occurrence had no correlation with cam location for the +0.35 mm contour (ρ = 0.04) and a moderate correlation for the +1 mm contour (ρ = 0.41, Fig. 9B).

Cam extent had a moderate to high positive correlation with

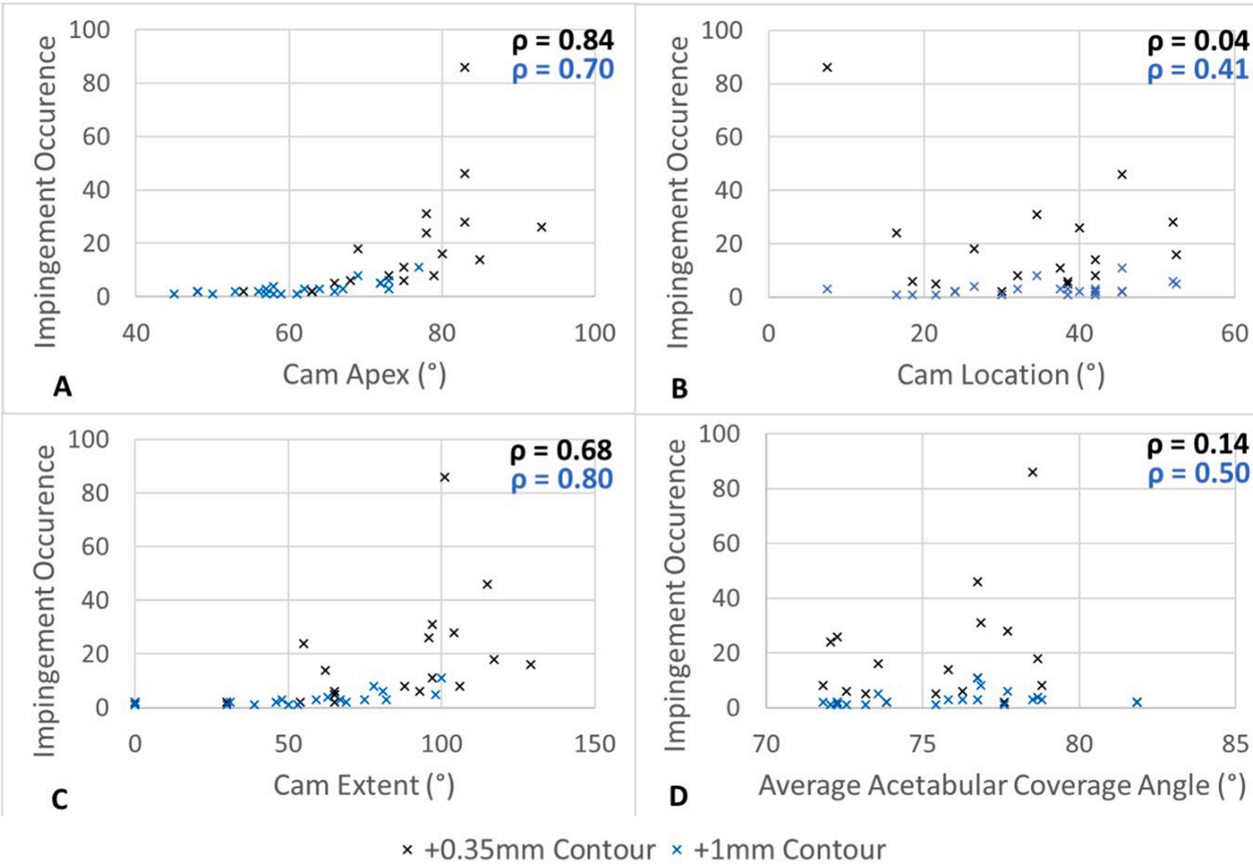

Fig. 9. Impingement occurrence (out of 126) for the +0.35 mm and +1 mm contour spheres vs: A) A subjects cam apex, B) cam location, C) cam extent at a threshold angle of 50°, D) a subjects average acetabular coverage angle. ρ = spearman's rank coefficient.

impingement occurrence for both the +0.35 mm and +1 mm contours (ρ = 0.68 and 0.80 respectively), with the higher impinging subjects displaying a larger area around the femoral head-neck junction of angles above 50° (Fig. 9C).

Impingement occurrence for the +0.35 mm contour had no correlation with acetabular coverage (ρ = 0.14), whilst impingement occurrence for the +1 mm contour showed a moderate positive correlation with acetabular coverage (ρ = 0.50) (Fig. 9D).

Discussion

This work has developed a contour method for describing the shape and height of cam lesions beyond their leading edge. This description provides both a richer visualisation of the cam shape and the ability to extract quantitative shape measures beyond the largest alpha angle. Application of joint motion across a range of activities allowed for prediction of impingement severity measures and an assessment of their potential use for prediction of damage severity across different subjects. Finally, the shape measures were compared to impingement severity, for better understanding of impingement mechanisms.

Cam contour shape description

The 20 cam lesions in this work were located predominantly in the superior-anterior portion of the femur, consistent with previous reports [3]. The range of maximum alpha angles (measured as the cam apex angle of the +0.35 mm contour, 47°−98°) was consistent with the range previously reported for a symptomatic cam-type hip population (45°−95°) [9]. Previous studies, recording mean alpha angles or extent measurements, typically found values that fall between those found here close to a sphere of best fit (+0.35 mm contour) and those taken at a cam height of 1 mm. For the mean cam alpha angle, previous studies reported between 66° and 74° [9,16,17], where the +0.35 mm contour average was 75° and the +1 mm contour average was 61° For the cam extent, a previous study reported a mean of 65° [5] (using the same threshold angle of 50° as used here), falling between the +0.35 mm contour average of 80° and the +1 mm contour average of 53° Therefore, the first two contours contain the shape features which are typically captured in a clinical context. Not all of the maximum alpha angles recorded in this study (Subject 20, 47°) meet the threshold of what is typically considered indicative of cam-type FAIS (ranging from 50°−60°, [4,18]) highlighting the current lack of consensus of what constitutes a pathological alpha angle.

Impingement severity measures over multiple height contours

There was a spread of impingement occurrence results across the 20 subjects (from 5 to 94, out of 630), demonstrating potential for use of that measure to differentiate the severity of cam impingement. The ability to analyse impingement occurrence over multiple height contours adds value, as subjects could be further differentiated by the occurrence at the +1 mm and +2 mm contours.

Both the occurrence data and the impingement visualisation show that the majority of impingement is recorded for the +0.35 mm and +1 mm contours. If the cam height contours passing into the acetabular socket can be translated into a restriction of the joint space, then the predicted impingement indicated less than 1 mm of restriction for 10 subjects, less than 2 mm for eight subjects, and greater than 2 mm for just two subjects. Therefore, a reduction of joint space of no more than 25 % of a healthy joint is indicated for half of the group. However, a 1 mm restriction may be more important in advanced stages of joint degeneration due to joint space narrowing, with reported joint spaces of ≤ 2 mm [19,20].

The average maximum impingement depths (indicating incursion of the cam into the acetabular socket and ranging from 2 to 5 mm) are more sensitive to the overall precision of the model compared to the impingement occurrence. The model precision would need to be reviewed to establish whether subjects can be differentiated using this metric, given the small depth range and relatively large standard deviations. Factors that could currently be targeted for improvement without a change to the source imaging, include the number of points around the femoral neck and the density of contours describing the change in height moving over the head-neck junctions. The overall average impingement depth of 3 mm indicates that less of the cam lesion enters the acetabulum than might be expected for this symptomatic group. This finding is in line with the theory of progression of soft tissue damage in cam-type FAIS; that initially starts at the acetabular edge as a mild chondrolabral injury [4].

Relationships between shape measures and impingement occurrence

Both cam apex angles and cam extent were positively correlated with impingement occurrence. Some previous studies have found that larger cam alpha angles produce more severe cartilage damage [16] while others found no correlation [6]. The correlation of cam extent with impingement occurrence suggests a greater spread of the cam the femoral neck junction also increases the risk of impingement. The complexity and variation in cam shape, even when only considering the leading edge, explains the challenge in correlating impingement damage to just one shape factor.

The location of the cam was weakly positively correlated with impingement occurrence, for the +1 mm height contour only. Previous work demonstrated differences in impingement occurrence for anteriorly versus superiorly located cam lesions [10]. However, that study used idealised shape cases where the location of the cam was varied in isolation, holding the cam size and extent and the acetabular rim shape constant. The current work has demonstrated that any effect that cam location may have on impingement occurrence is hard to detect statistically where subject-specific hip shapes are used, as there are more confounding factors.

Acetabular coverage had a moderate positive correlation with impingement occurrence at the +1 mm height contour. This suggests that greater acetabular coverage may increase the risk of impingement with greater heights of the cam lesion, implying greater restriction of the joint space. Severity of FAIS is understood to be increased with a larger cam lesion and with higher acetabular coverage [21]. The latter is typically thought to induce “pincer” impingement, in which the acetabular labrum and rim abuts directly with the femoral neck. The current shape model is not designed with pincer impingement in mind, but is focused on cam impingement, represented by the incursion of the cam lesion into the acetabular socket. The introduction of height contour mapping in this work illustrates the role of acetabular coverage in cam impingement, in the absence of a pincer mechanism.

Limitations and future development

The contour method provided data on the height of cam involved in restricting the joint space. However, the volume of cam involved in the impingement has been previously correlated with damage [6] but was not explicitly recorded in this study, and therefore remains an aspect of future work.

In the current work, bone boundaries can be identified to within 0.5 mm, given the image resolution. This uncertainty, along with that caused by the segmentation process, is of most concern when identifying the lowest height contours, where cam geometry could be most confounded by femoral head shape variations. A future piece of work will quantify that uncertainty and make recommendation on image resolution and process automation.

This study assumed the same joint alignment for all subjects. Not using subject-specific hip alignment may result in over or under predicting a subject’s impingement occurrence and depth, and affect impingement location prediction. This method allows for an assessment of whether the model generates a range of impingement outputs based solely on hip shape. However, subject-specific alignment would be needed to make comparisons to clinically observed impingement damage [10,22]. The sensitivity of the impingement occurrence to coronal and axial joint orientation and pelvic tilt were previously tested [10]. A neutral standing pelvic tilt is likely to be difficult to establish for a specific patient as imaging is typically done in a supine position. However, impingement occurrence was least sensitive to pelvic tilt [10].

The geometry captured to represent the acetabulum was that of the bony rim and therefore this study does not explicitly consider the impingement of the cam with the labrum and cartilage compression [10]. Results in this study indicate potential for soft tissue damage through the prediction of bone-on-bone impingement, supported by recent studies into FAIS [3].

Hip motion data was collected from individuals in the general population who were not diagnosed with cam-type FAIS [10]. Therefore, individual shape-motion combinations may not be realistic and should not be over-interpreted. This was addressed in this work through a high-level statistical approach to impingement occurrence and the removal of data subsets with less than 3 instances of impingement for the calculation of impingement depth. Future refinement of the motion data to match the age profile of the subjects in this study would allow for relationships between specific movement types and impingement occurrence to be assessed.

Joint contact forces were not considered in the mathematical shape-motion model, only joint motion was assessed, limiting the evaluation of impingement severity to impingement occurrence and depth. Consideration of joint contact force is likely to be needed for direct prediction of soft tissue damage.

Conclusion

This work has demonstrated the value of capturing the progressive height of cam lesions on the femoral head-neck junction. Typical clinical alpha angle measurements were contained by the two leading edge, lowest height contours. The remaining contours captured the progression of cam lesion height, further from the articulating surface. The majority of predicted impingement across the 20 hip shape subjects did not reach those higher contours, indicating that some areas considered to be part of the cam may not be involved the impingement. Therefore, it is possible that adequate resection of the first 1 mm of cam height is the most critical in reducing a subject’s impingement severity.

The shape-motion model predicts occurrence of impingement across a broad set of activity-based motions. Results provided encouragement for the use of this metric as it generated a spread of values over the 20 subjects and had some correlation with established shape metrics (namely alpha angles and extent of the cam lesion).

The lack of strong correlation with any single shape measure supports the use of a modelling tool which sufficiently captures the complex shape and generates an impingement risk metric which also accounts for joint motion.

Funding

This research was funded by the University of Leeds. Jones was supported by the Royal Academy of Engineering under the Leverhulme Trust Research Fellowship scheme. Williams is supported by Royal Academy of Engineering, DePuy Synthes Chair.

CRediT authorship contribution statement

Trent Edward Rayment: Writing – review & editing, Writing – original draft, Visualization, Validation, Software, Project administration, Methodology, Investigation, Formal analysis, Data curation, Conceptualization. **Sophie Williams:** Writing – review & editing, Supervision, Methodology, Funding acquisition, Conceptualization. **Alison Claire Jones:** Writing – review & editing, Visualization, Validation, Supervision, Software, Resources, Project administration, Methodology, Funding acquisition, Formal analysis, Data curation, Conceptualization.

Declaration of competing interest

The authors declare that they have no known competing financial interests or personal relationships that could have appeared to influence the work reported in this paper.

Data availability

The data associated with this study is openly available from the University of Leeds Data Repository.

Acknowledgements

The authors would like to thank Mr. Colin Holton at Leeds Teaching Hospitals NHS Trust for his insight into current clinical practises and Mr Marcus Bankes for his contribution of the subject CT image data.

References

[1] R. Ganz, J. Parvizi, M. Beck, M. Leunig, H. Nötzli, K.A. Siebenrock, Femoroacetabular impingement: a cause for osteoarthritis of the hip, Clin. Orthop. Relat. Res.® 417 (2003) 112–120, https://doi.org/10.1097/01.blo.0000096804.78689.c2.

[2] Non-arthroplasty hip registry. Available at: https://www.nahr.co.uk/. Accessed 21 September 2023.

[3] C. Pascual-Garrido, D.J. Li, G. Grammatopoulos, E.L. Yanik, J.C. Clohisy, The pattern of acetabular cartilage wear is hip morphology-dependent and patient demographic-dependent, Clin. Orthop. Relat. Res.® 477 (5) (2019) 1021, https://doi.org/10.1097/CORR.0000000000000649.

[4] T.L. Johnston, M.L. Schenker, K.K. Briggs, M.J. Philippon, Relationship between offset angle alpha and hip chondral injury in femoroacetabular impingement, Arthroscopy: J. Arthrosc. Relat. Surg. 24 (6) (2008) 669–675, https://doi.org/10.1016/j.arthro.2008.01.010.

[5] V.V. Mascarenhas, P. Rego, P. Dantas, A. Gaspar, F. Soldado, J.G. Consciência, Cam deformity and the omega angle, a novel quantitative measurement of femoral head-neck morphology: a 3D CT gender analysis in asymptomatic subjects, Eur. Radiol. 27 (5) (2017) 2011–2023, https://doi.org/10.1007/s00330-016-4530-0.

[6] R. Dessouky, A. Chhabra, L. Zhang, A. Gleason, R. Chopra, Y. Chatzinoff, N.P. Fey, Y. Xi, J. Wells, Cam-type femoroacetabular impingement-correlations between alpha angle versus volumetric measurements and surgical findings, Eur. Radiol. 29 (7) (2019) 3431–3440, https://doi.org/10.1007/s00330-018-5968-z.

[7] M. Guidetti, P. Malloy, T.D. Alter, A.C. Newhouse, A.A. Espinoza Orías, N. Inoue, S. J. Nho, MRI– and CT–based metrics for the quantification of arthroscopic bone resections in femoroacetabular impingement syndrome, J. Orthop. Res. 40 (5) (2022) 1174–1181, https://doi.org/10.1002/jor.25139. May Epub 2021 Jul 12. PMID: 34192370.

[8] R.W. Kang, A.B. Yanke, A.A. Espinoza Orias, N. Inoue, S.J. Nho, Emerging ideas: novel 3-D quantification and classification of cam lesions in patients with femoroacetabular impingement, Clin. Orthop. Relat. Res. 471 (2) (2013) 358–362, https://doi.org/10.1007/s11999-012-2693-9. FebEpub 2012 Nov 6. PMID: 23129477; PMCID: PMC3549194.

[9] M.T. Milone, A. Bedi, L. Poultsides, E. Magennis, J.W.T. Byrd, C.M. Larson, B. T. Kelly, Novel CT-based three-dimensional software improves the characterization of cam morphology, Clin. Orthop. Relat. Res.® 471 (8) (2013) 2484–2491, https://doi.org/10.1007/s11999-013-2809-x.

[10] A.C. Jones, T.D. Stewart, N. Maher, C. Holton, Can a computational model predict the effect of lesion location on cam-type hip impingement? Clin. Orthop. Relat. Res.® 481 (7) (2023) 1432–1443, https://doi.org/10.1097/CORR.0000000000002565.

[11] R.J. Cooper, M. Mengoni, D. Groves, S. Williams, M.J.K. Bankes, P. Robinson, A. C. Jones, Three-dimensional assessment of impingement risk in geometrically parameterised hips compared with clinical measures, Int. J. Numer. Method Biomed. Eng. . 33 (11) (2017) e2867, https://doi.org/10.1002/cnm.2867.

[12] M. Lequesne, J. Malghem, E. Dion, The normal hip joint space: variations in width, shape, and architecture on 223 pelvic radiographs, Ann. Rheum. Dis. 63 (9) (2004) 1145–1151, https://doi.org/10.1136/ard.2003.018424.

[13] R.B. Layton, N. Messenger, T.D. Stewart, Analysis of hip joint cross-shear under variable activities using a novel virtual joint model within Visual3D, Proc. Inst. Mech. Eng. H 235 (10) (2021) 1197–1204, https://doi.org/10.1177/0954411921102586.

[14] A. Jones. Human Hip Joint Impingement Shape and Motion model: Input and Output Data For an Initial Study of Eight Typical Cam-Type Hips. Univ. of Leeds. Available at: https://doi.org/10.5518/1231.

[15] T.E. Rayment, D. Groves-Williams, S. Williams, A.C. Jones, Twenty Cam-Type Hip Shapes Described Using a New 'contour' Shape Map Assessed For Impingement Occurrence and Depth, Univ. of Leeds, 2024, https://doi.org/10.5518/1492 [Dataset].

[16] P.E. Beaulé, K. Hynes, G. Parker, K.A. Kemp, Can the alpha angle assessment of cam impingement predict acetabular cartilage delamination? Clin. Orthop. Relat. Res.® 470 (12) (2012) 3361–3367, https://doi.org/10.1007/s11999-012-2601-3.

[17] H.P. Nötzli, T.F. Wyss, C.H. Stoecklin, M.R. Schmid, K. Treiber, J. Hodler, The contour of the femoral head-neck junction as a predictor for the risk of anterior impingement, J. Bone Jt. Surg. Br. 84-B (4) (2002) 556–560, https://doi.org/10.1302/0301-620x.84b4.12014. Vol.

[18] P.R. Atkins, Y. Shin, P. Agrawal, S.Y. Elhabian, R.T. Whitaker, J.A. Weiss, S. K. Aoki, C.L. Peters, A.E. Anderson, Which two-dimensional radiographic measurements of cam femoroacetabular impingement best describe the three-dimensional shape of the proximal femur? Clin. Orthop. Relat. Res. 477 (1) (2019) 242–253, https://doi.org/10.1097/CORR.0000000000000462. JanPMID: 30179924; PMCID: PMC6345307.

[19] C.M. Larson, M.R. Giveans, M. Taylor, Does Arthroscopic FAI correction improve function with radiographic arthritis? Clin. Orthop. Relat. Res.® 469 (6) (2011) 1667–1676, https://doi.org/10.1007/s11999-010-1741-6.

[20] A. Nehme, G. El-Hajj, J. Maalouly, R. Ayoubi, H. Abdel-Nour, R. Moucharafieh, R. Ashou, Hip joint space width in an asymptomatic population: computed tomography analysis according to femoroacetabular impingement morphologies, Asia-Pac. J. Sports Med., Arthrosc., Rehabil. Technol. 24 (2021) 14–22, https://doi.org/10.1016/j.asmart.2021.01.001.

[21] J. Cobb, K. Logishetty, K. Davda, F. Iranpour, Cams and pincer impingement are distinct, not mixed: the acetabular pathomorphology of femoroacetabular impingement, Clin. Orthop. Relat. Res.® 468 (8) (2010) 2143–2151, https://doi.org/10.1007/s11999-010-1347-z.

[22] C.Y.W. Heimer, C.H. Wu, C. Perka, S. Hardt, F. Göhler, T. Winkler, H.C. Bäcker, The impact of hip dysplasia on CAM impingement, J. Personalized Med. 12 (7) (2022) 1129, https://doi.org/10.3390/jpm12071129.